XV INTERNATIONAL SUMMER SCHOOL NICOLÁS CABRERA

100 YEARS LIQUID HELIUM: NEW PHYSICS AT THE EDGE OF ABSOLUTE ZERO

14-19 September 2008

Superfluid 3He in aerogel

I.A. Fomin,

P.L. Kapitza Institute for Physical Problems, Moscow.

Helium = ^{4}He-isotope
2 protons+2 neutrons
$T_{boiling}$=4.2 K
$\rho = 0.145 g/cm^3$

^{3}He – 2 protons+1 neutron
$T_{boiling}$=3.69 K
$\rho = 0.08 g/cm^3$

At $T_\lambda = 2.17K$ 4He becomes superfluid.

This ordering is characterized by the order parameter

$$\psi = |\psi| e^{i\varphi} \qquad \mathbf{v}_s = \frac{\hbar}{m} \nabla \varphi$$

gauge symmetry is broken

At $T \sim 1K$ liquid ^{3}He is a normal Fermi liquid, it can became superfluid via Cooper pairing at lower temperatures.

Singlet Cooper pairing

S=0, l=0

S=0 *l*= 0,2,4…

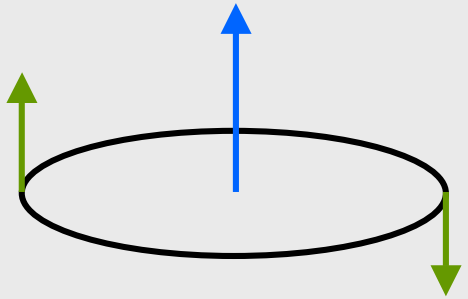

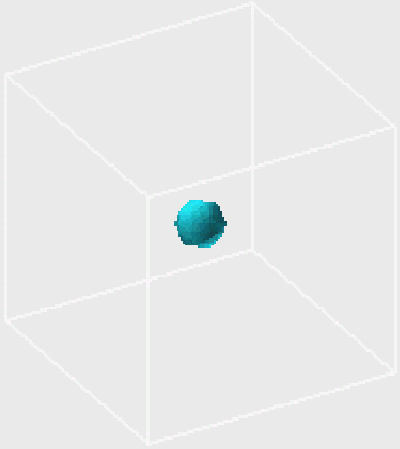

S=0, l=0 s-wave, or *conventional* Cooper pairing. It is realized in most of superconductors: Hg, Pb, Sn, Al, etc..
The order parameter is a one-component complex function:

$$\Psi = |\Psi| e^{i\phi}$$

only gauge symmetry is broken.

Triplet Cooper pairing (*unconventional)*

S=1 l=1,3,5…

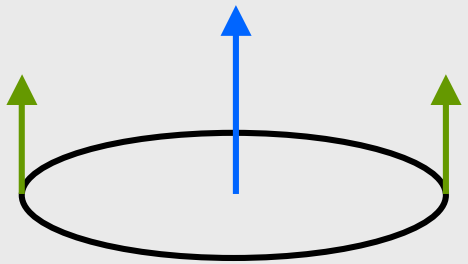

$$\Psi = \begin{pmatrix} \psi_{\uparrow\uparrow} \\ \frac{1}{\sqrt{2}}(\psi_{\uparrow\downarrow} + \psi_{\downarrow\uparrow}) \\ \psi_{\downarrow\downarrow} \end{pmatrix}$$

The order parameter is multi-component:

Ψ_x, Ψ_y, Ψ_z. Each of the three components is a function of direction in the momentum space.

Except for the gauge symmetry other symmetries are broken as well.

The order parameter of ^{3}He: s=1, l=1

$$\Psi_\mu = \Sigma A_{\mu j} k_j$$

momentum (orbital) index
j=1,2,3 - px,py,pz orbitals

$A_{\mu j}$

spin index μ = 1,2,3

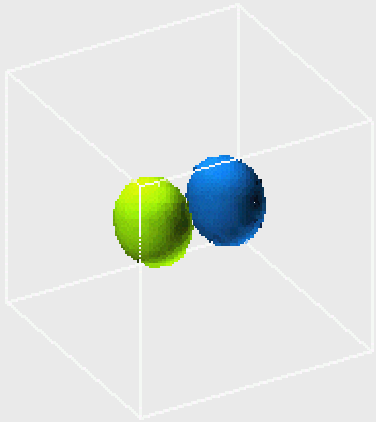

px

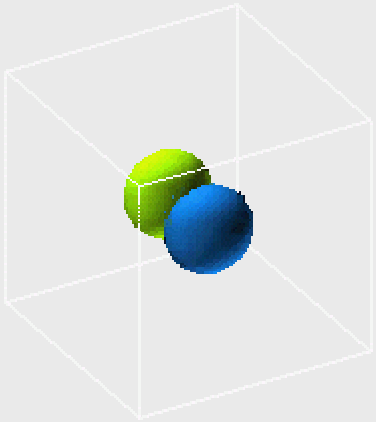

py

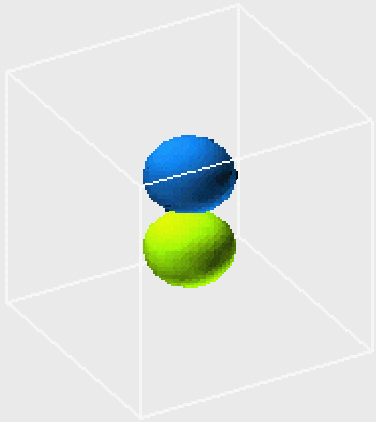

pz

Cooper pairing in a triplet (S=1) state

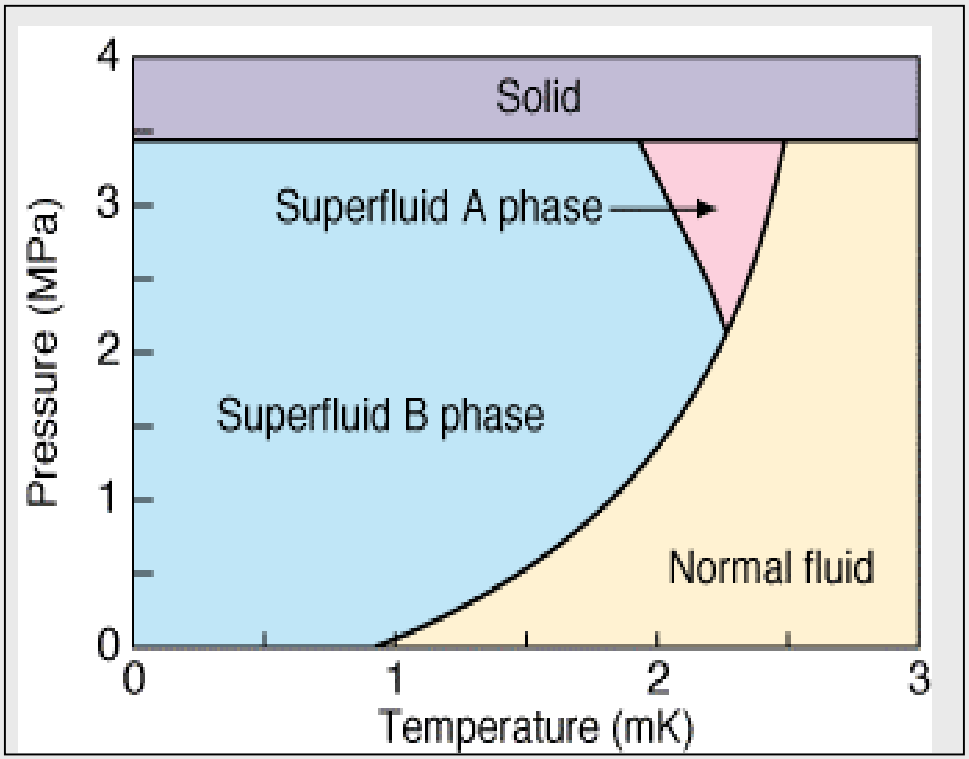

$$A^{ABM}_{\mu j} = \Delta \frac{1}{\sqrt{2}} \hat{d}_\mu (\hat{m}_j + i\hat{n}_j),$$

$$A^{BW}_{\mu j} = \Delta \frac{1}{\sqrt{3}} e^{i\varphi} R_{\mu j}.$$

Unconventional superconductors:

UPt_3, UGe_2, Sr_2RuO_4, high-T_c, etc.

Additional complications: anisotropy, complicated Fermi-surfaces, *impurities.*

^3He – canonical unconventional superfluid: spherical Fermi-surface, well known Fermi-liquid parameters, *no impurities*.

All floating impurities stick to the walls of a container.

Self-supporting structure – high porosity silica aerogel.

[1] J. V. Porto and J. M. Parpia, *Phys. Rev. Lett.*, **74**, 4667 (1995)

[2] D. T. Sprague,T. M. Haard,J. B. Kycia, V. R. Rand, Y. Lee, P. Hamot and W. P. Halperin, *Phys. Rev. Lett.*, **75**, 661 (1995)

Porosity *P=*
(empty volume/total volume)

Aerogels with the porosity up to 99.5% can be made.

Mostly used with the porosity close to 98%

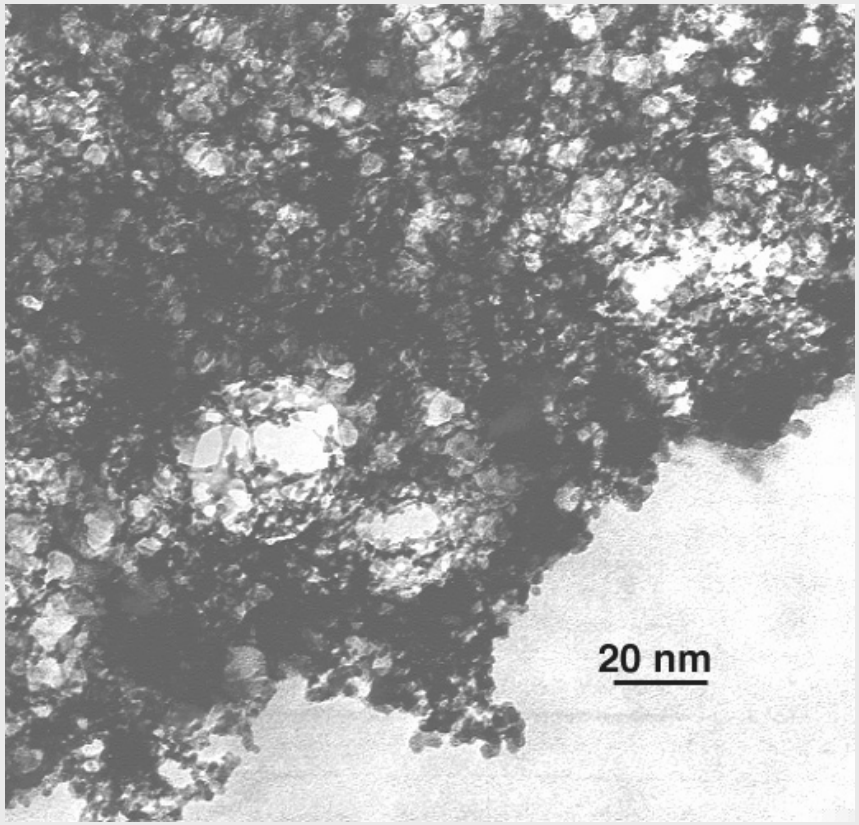

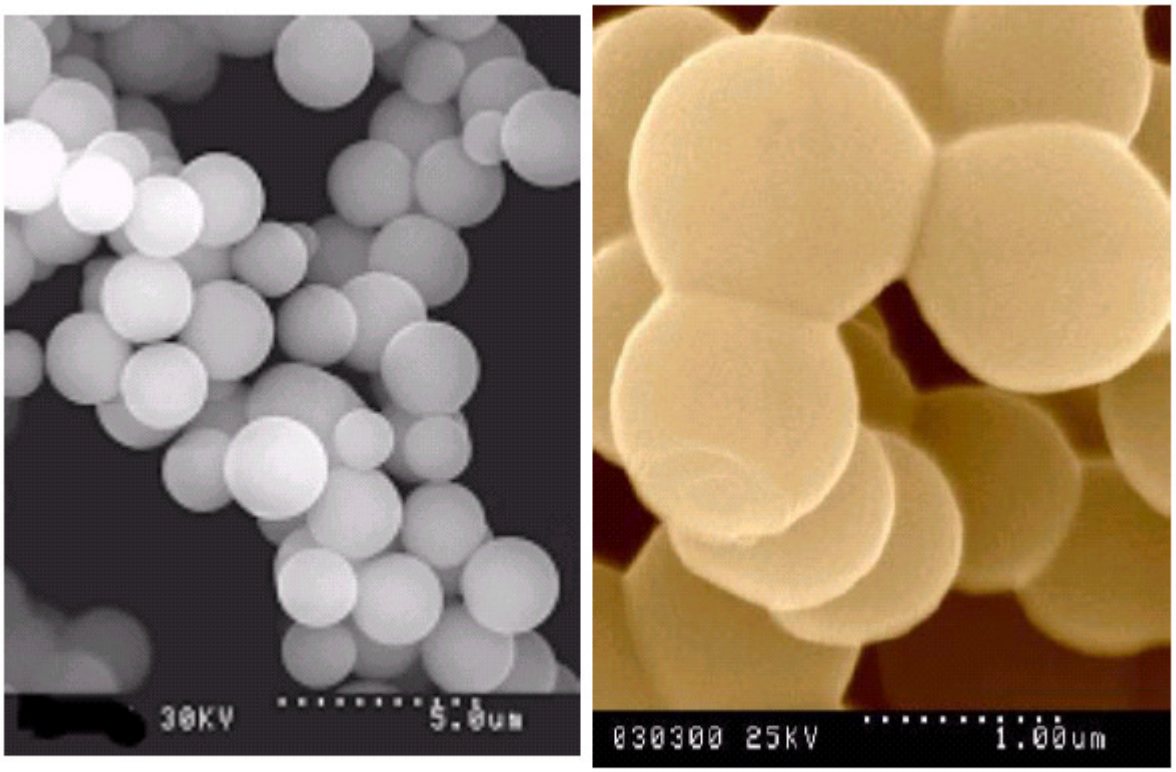

Fig 3. SEM micrographs of porous silica aerogel microparticles.

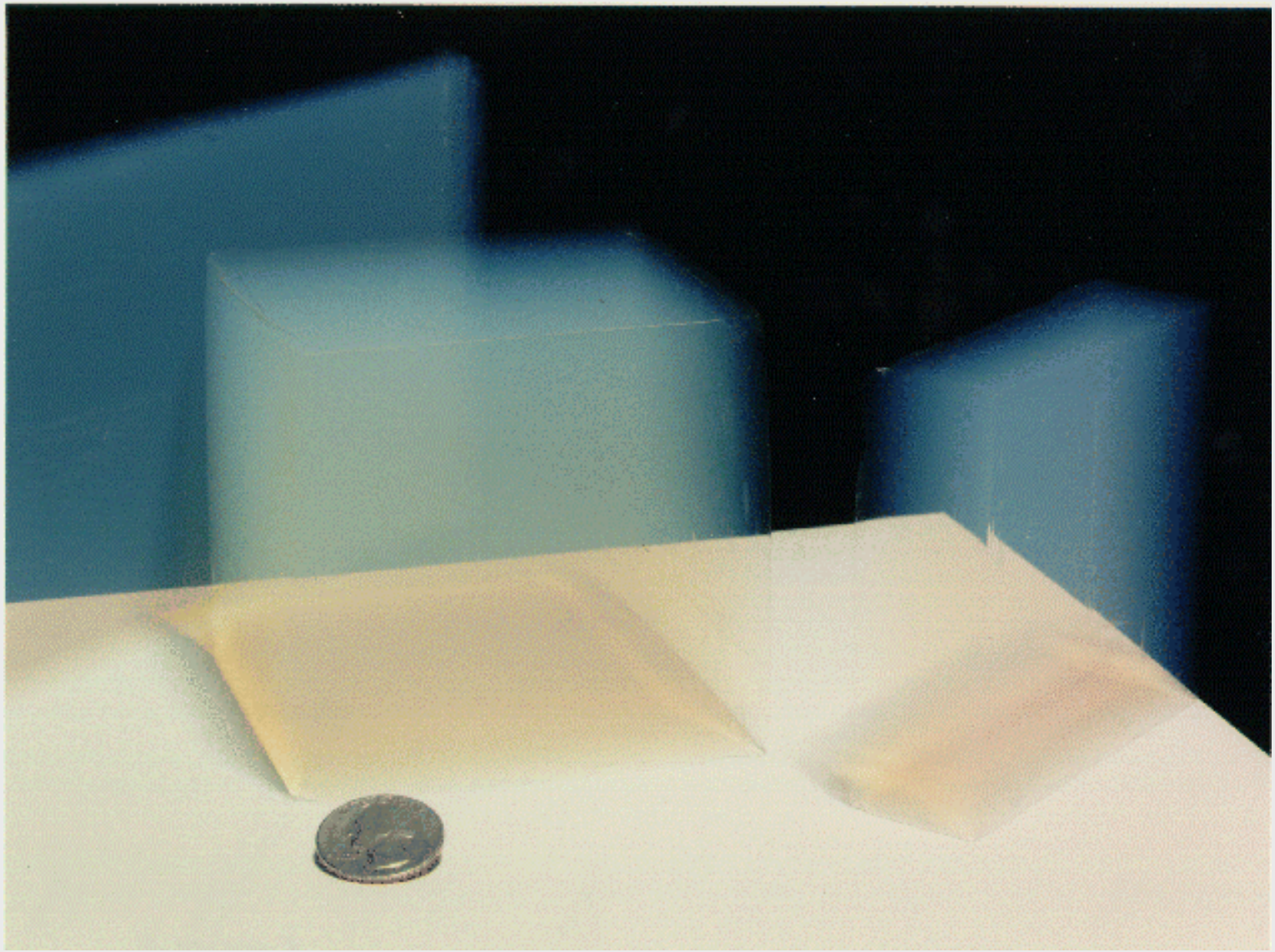

Fig 1. A 2.5 kg brick is supported on top of a piece of aerogel weighing only 2.38 g. (NASA)

Why Aerogel?

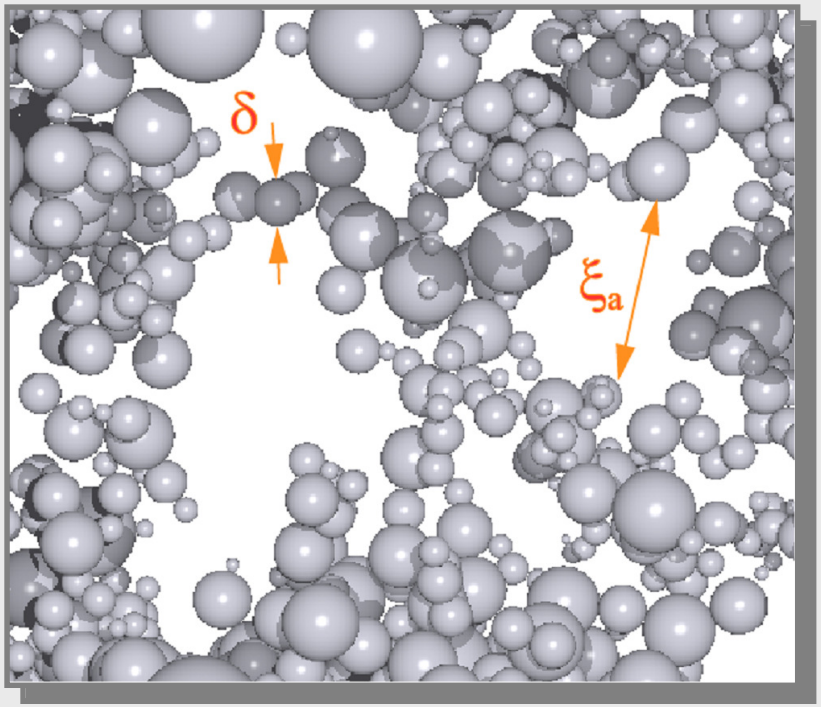

DLCA simulation of a silica aerogel depicting the length scales δ and ξ_a (courtesy of T.M. Lippman).

- Silica ball size:

  $\delta \approx 3$ nm
- Correlation length:

  $\xi_a \sim 10 - 100$ nm
- Superfluid coherence length:

  $\xi \approx 20 - 80$ nm (P = 34 - 0 bar)
- Expect interesting physics when: $\xi \sim \xi_a$

How does aerogel effect the Tc of 3He?

According to the theory of superconducting alloys

A.A. Abrikosov and L.P. Gorkov, *ZhETF* **39**, 1781 (1961), [*Sov. Phys. JETP* **12**, 1243 (1961)].

for conventional superconductors $T_c \approx T_c^0$

for unconventional

$$\frac{T_c^0 - T_c}{T_c^0} \sim \frac{\xi_0}{l_{tr}}$$

$$\xi_0 = \frac{\hbar v_F}{2\pi T_c}$$

A. I. Larkin, *ZhETF*, **58**, 1466 (1970) [Sov. Phys. JETP, **31**, 784 (1970)]

Application of the Theory of superconducting alloys for a triplet p-wave Cooper pairing (Homogenious Scattering Model (HSM))

E.V. Thuneberg, S.-K. Yip, M. Fogelstrom, and J.A. Sauls, *Phys. Rev. Lett.*, **80**, 2861 (1998)

$$\ln\frac{T_c^0}{T_c} = \psi\left(\frac{1}{2}+\frac{\xi_0}{2l_{tr}}\frac{T_c^0}{T_c}\right) - \psi\left(\frac{1}{2}\right)$$

$$\psi(z) = \frac{d}{dz}\ln\Gamma(z)$$

$$\frac{T_c^0 - T_c}{T_c^0} \approx \frac{\pi^2}{4}\frac{\xi_0}{l_{tr}}$$

$$\xi_0 = \frac{\hbar v_F}{2\pi T_c^0}$$

Suppression of T_c

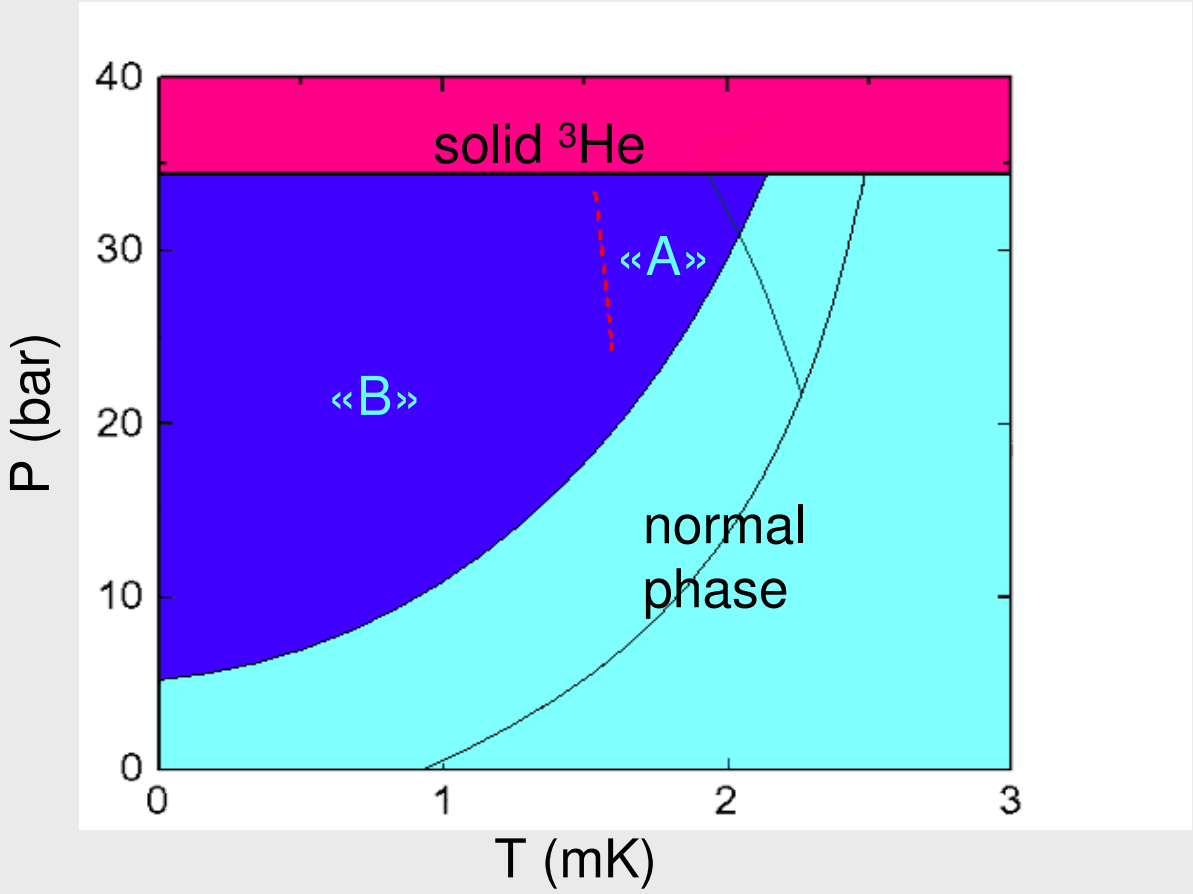

$$\frac{T_c^0 - T_c}{T_c^0} \approx \frac{\pi^2}{4}\frac{\xi_0}{l_{tr}}$$

$$\xi_0 = \frac{\hbar v_F}{2\pi T_c^0}$$

Compare suppression to model of point magnetic scatterers in s-wave superconductors

Abrikosov-Gorkov – homogenous scattering model

$$\ln\left(\frac{T_c}{T_c^0}\right) = \Psi\left(\frac{1}{2}\right) - \Psi\left(\frac{1}{2} + \frac{\xi_0}{4l}\frac{T_c^0}{T_c}\right)$$

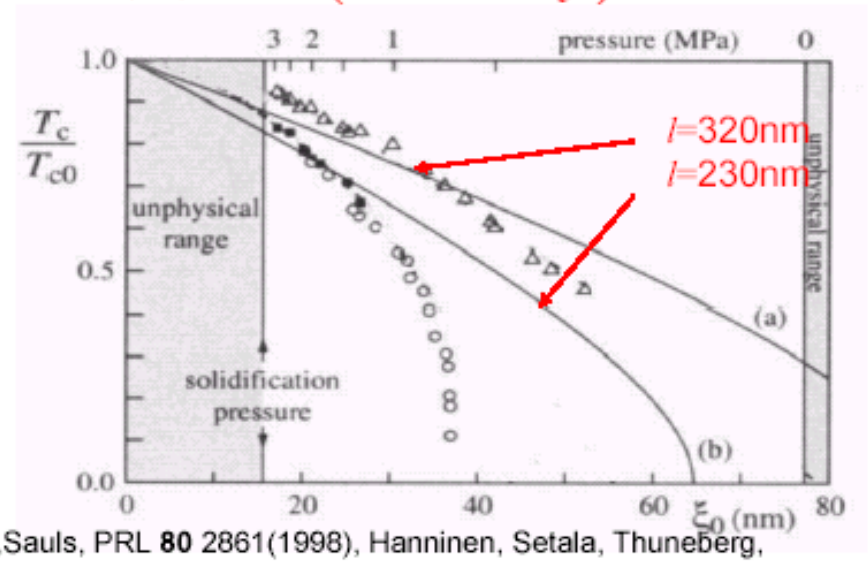

Thuneberg,Yip,Fogelstrom,Sauls, PRL **80** 2861(1998), Hanninen, Setala, Thuneberg, Physica B, **255** 11 (1999),

$$(T^0 - T_c)/T_c^0 \sim \xi_0/l_{tr}$$

Homogenious scattering model

ξ_0

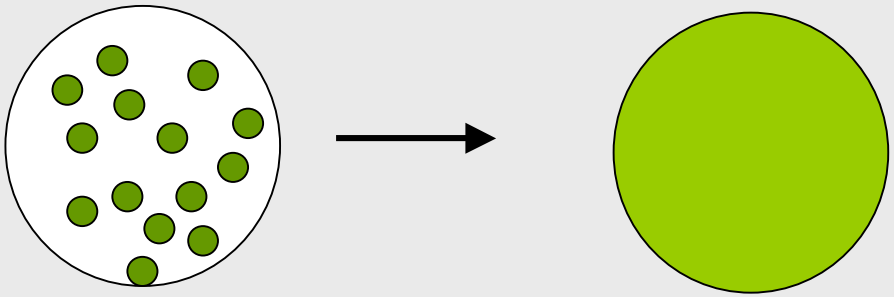

$$\exp\left(-\frac{i\xi t}{\hbar}\right) \rightarrow \exp\left(-\frac{i\xi t}{\hbar} - \frac{\gamma t}{\hbar}\right)$$

$$\frac{\hbar}{\gamma} = \tau = \frac{l}{v}$$

$$\ln\frac{T_c^0}{T_c} = \psi\left(\frac{1}{2} + \frac{\xi_0}{2l_{tr}}\frac{T_c^0}{T_c}\right) - \psi\left(\frac{1}{2}\right)$$

W.F. Halperin and J.A. Sauls, cond-mat/0408593

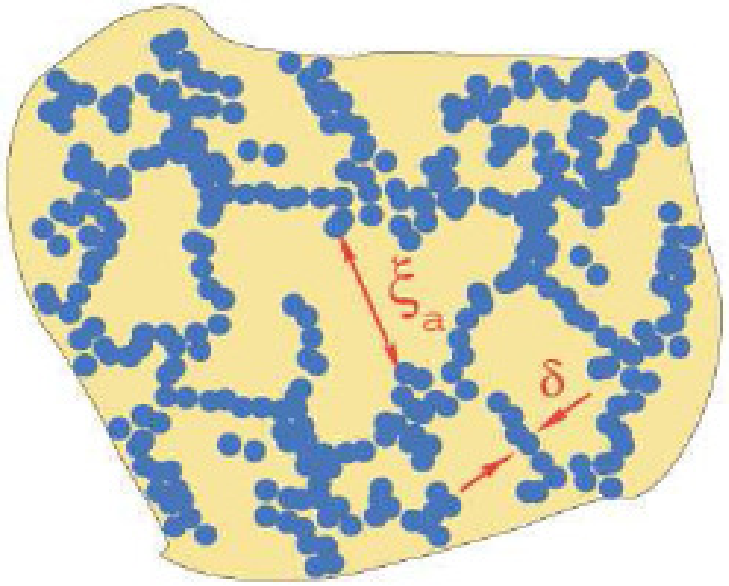

FIG. 4: A sketch of silica aerogel showing low-density regions containing ^{3}He (yellow) threaded by higher density strands and aggregates of silica (blue). Two principal length scales are indicated: the typical size of the aerogel strands, $\delta \simeq 3\,\mathrm{nm}$, and the aerogel correlation length, $\xi_a \simeq 30\,\mathrm{nm}$, identified as the average inter-strand distance.

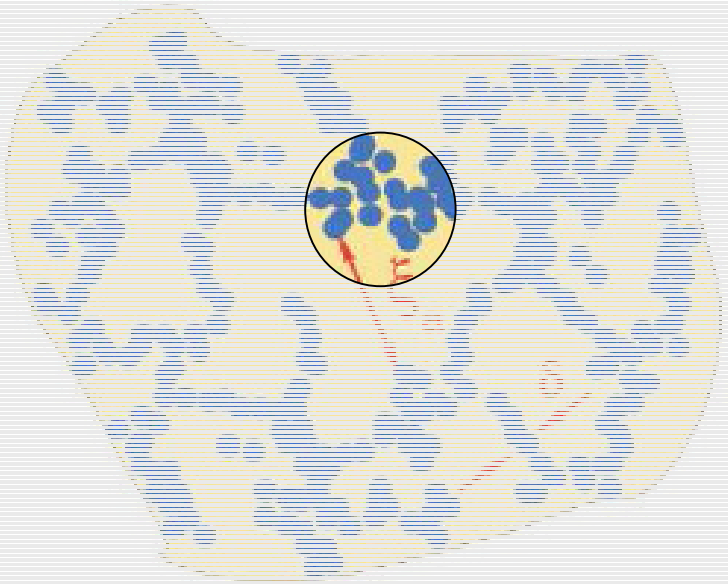

FIG. 1. A sketch of silica aerogel showing low-density regions containing gas (yellow) threaded by higher-density strands and aggregates of silica (blue). Two principal length scales are indicated: the typical size of the aerogel strands, $\delta \sim 3\,\mathrm{nm}$, and the aerogel correlation length, $\xi_a \simeq 30\,\mathrm{nm}$, identified as the average inter-strand distance.

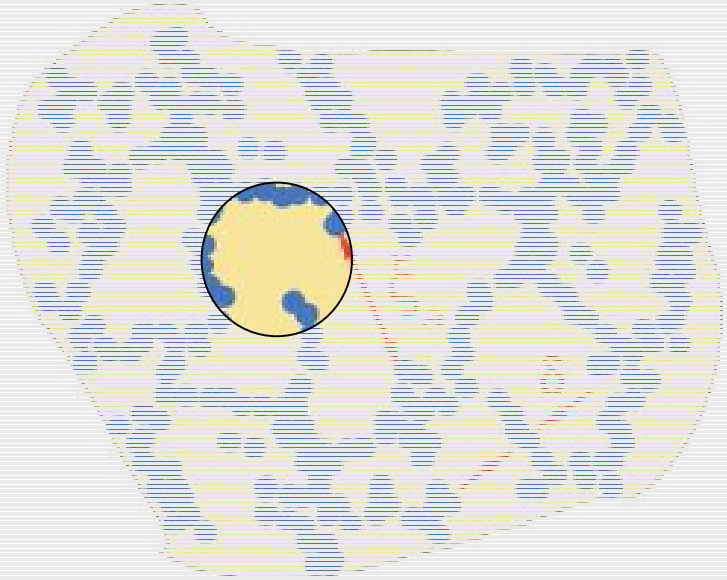

FIG. 4. A sketch of silica aerogel showing low-density regions containing ^3He (yellow) threaded by higher-density strands and aggregates of silica (blue). Two principal length scales are indicated: the typical size of the aerogel strands, $\lambda \sim 3\,\mathrm{nm}$, and the aerogel correlation length, $\xi_a \sim 30\,\mathrm{nm}$, identified as the average inter-strand distance.

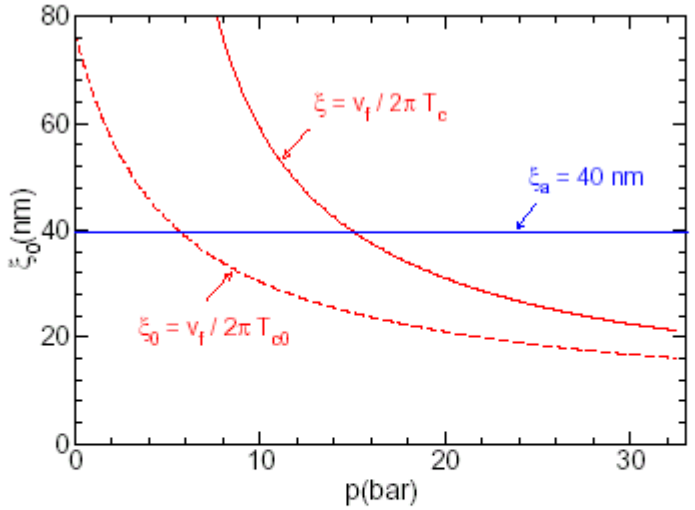

FIG. 2: The pair correlation length of superfluid ^{3}He in aerogel (solid curve) as a function of pressure is shown in comparison with an aerogel strand-strand correlation length, $\xi_a \simeq 40\,\mathrm{nm}$. A cross-over occurs near $p \approx 15\,\mathrm{bar}$. The bulk ^{3}He correlation length is also shown (dashed curve).

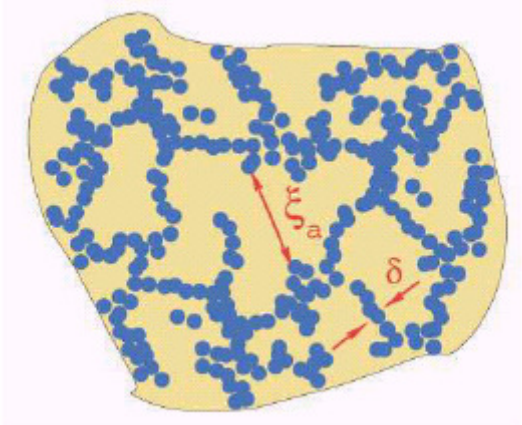

$$x = \frac{\xi_0}{l_{tr}} \frac{T_c^0}{T_c}$$

$$x \to \tilde{x} = \frac{x}{1 + \zeta_a^2 / x}$$

where $\zeta_a \equiv \xi_a / \ell$

$$\ln \frac{T_c^0}{T_c} = \psi\left(\frac{1}{2} + \frac{\xi_0}{2l_{tr}} \frac{T_c^0}{T_c}\right) - \psi\left(\frac{1}{2}\right)$$

Sharma & Sauls, PRB **68**224500 (2003)

When $\xi_{3He} >> \xi_a << l$ *(mfp)*,
$\delta T_c/T_{co} \sim -(\xi_{3He}/l)$.

When $\xi_{3He} \sim \xi_a << l$ *(mfp)*, T_c set by most dense regions
$\delta T_c/T_{co} \sim -(\xi_{3He}/\xi_a)^2$.

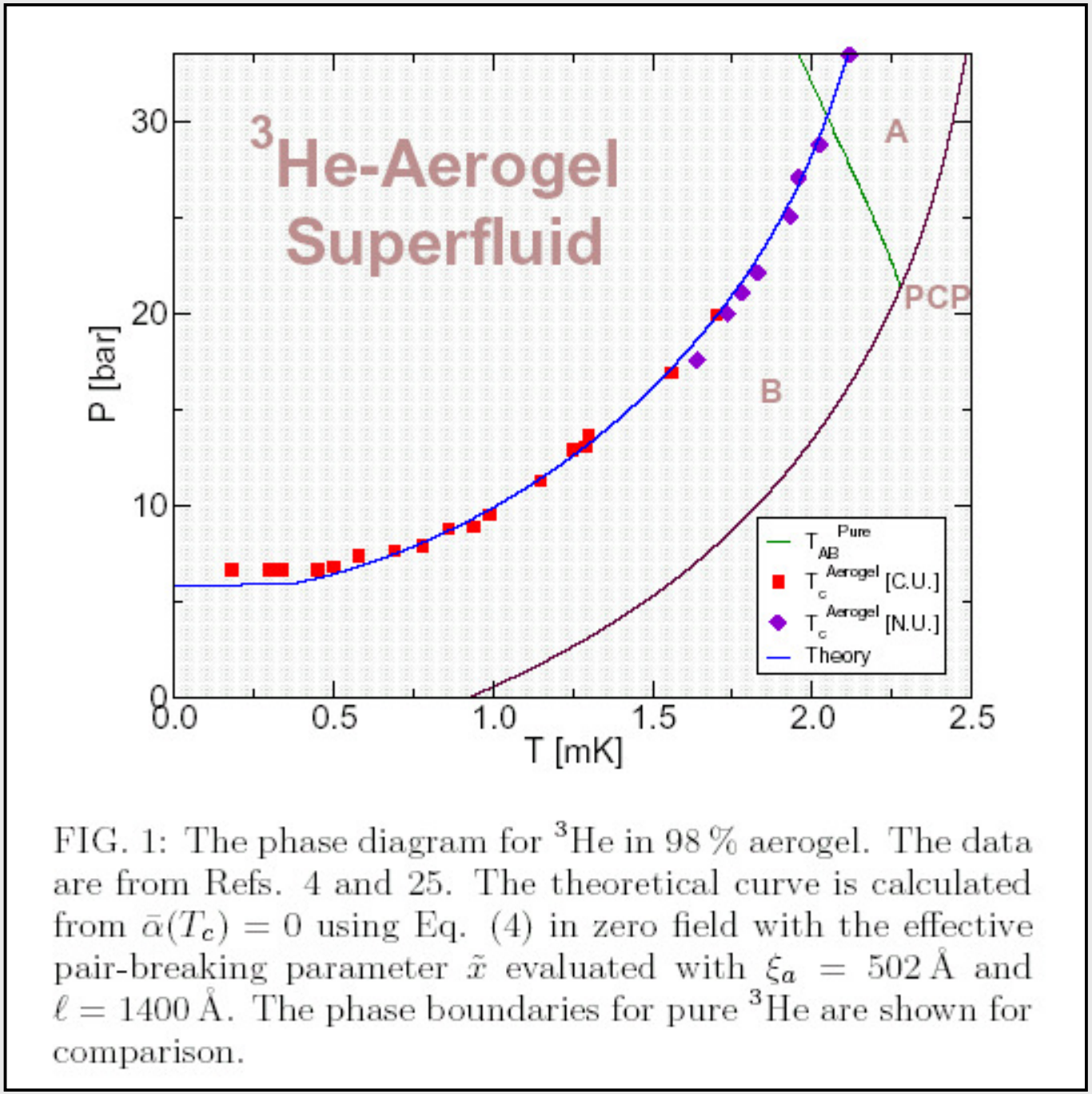

FIG. 1: The phase diagram for ^{3}He in 98 % aerogel. The data are from Refs. 4 and 25. The theoretical curve is calculated from $\bar{\alpha}(T_c) = 0$ using Eq. (4) in zero field with the effective pair-breaking parameter $\tilde{x}$ evaluated with $\xi_a = 502\,\text{Å}$ and $\ell = 1400\,\text{Å}$. The phase boundaries for pure ^{3}He are shown for comparison.

Landau free energy

$$f = f_n + \alpha A_{\mu j} A^*_{\mu j} + \beta_1 |A_{\mu j} A_{\mu j}|^2 + \beta_2 (A_{\mu j} A^*_{\mu j})^2 +$$

$$\beta_3 A^*_{\mu j} A^*_{\nu j} A_{\nu l} A_{\mu l} + \beta_4 A^*_{\mu j} A_{\nu j} A^*_{\nu l} A_{\mu l} + \beta_5 A^*_{\mu j} A_{\nu j} A_{\nu l} A^*_{\mu l}.$$

$$\frac{\partial f}{\partial A^*_{\mu j}} = 0$$

$$F_\eta = N(0) \int \eta_{jl}(\mathbf{r}) A_{\mu j} A^*_{\mu l} d^3 r$$

$$F_{GL} = N(0) \int d^3 r [\tau A_{\mu j} A^*_{\mu j} + \eta_{jl}(\mathbf{r}) A_{\mu j} A^*_{\mu l} + \frac{1}{2} \sum_{s=1}^{5} \beta_s I_s +$$

$$\frac{1}{2} \left(K_1 \frac{\partial A_{\mu l}}{\partial x_j} \frac{\partial A^*_{\mu l}}{\partial x_j} + K_2 \frac{\partial A_{\mu l}}{\partial x_j} \frac{\partial A^*_{\mu j}}{\partial x_l} + K_3 \frac{\partial A_{\mu j}}{\partial x_j} \frac{\partial A^*_{\mu l}}{\partial x_l} \right)],$$

$$-\tau A_{\mu j}+A_{\mu l}\eta_{lj}(\mathbf{r})-\frac{3}{5}\xi_s^2\left(\frac{\partial^2 A_{\mu j}}{\partial x_l^2}+2\frac{\partial^2 A_{\mu l}}{\partial x_l \partial x_j}\right)+\frac{1}{2}\sum_{p=1}^{5}\beta_p\frac{\partial I_p}{\partial A^*_{\mu j}}=0$$

$$\tau = (T_b - T)/T_b$$

Ginzburg and Landau equation

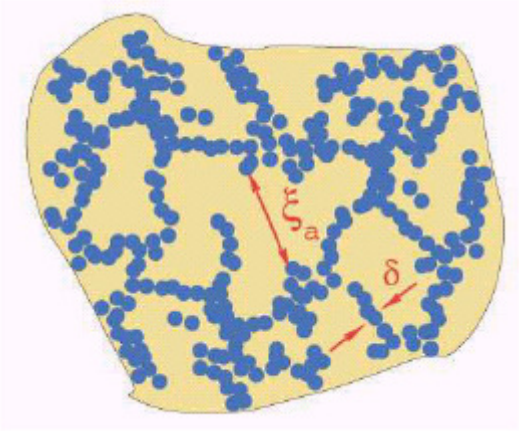

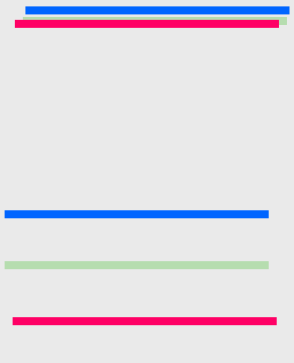

Tc

Tc1
Tc2
Tc3

Anisotropic part $\eta_{jl}^{(a)}(\mathbf{r}) \equiv \eta_{jl}(\mathbf{r}) - \frac{1}{3}\eta_{ll}(\mathbf{r})\delta_{jl}$ describes the local splitting of T_c for different projections of angular momenta caused by the local breaking of spherical symmetry by the aerogel strands.

$$-\tau A_{\mu j} + A_{\mu l}\eta_{lj}(\mathbf{r}) - \frac{3}{5}\xi_s^2\left(\frac{\partial^2 A_{\mu j}}{\partial x_l^2} + 2\frac{\partial^2 A_{\mu l}}{\partial x_l \partial x_j}\right) = 0$$

$$-\tau\psi(x) + \eta(x)\psi(x) - \xi_0^2\frac{d^2\psi}{dx^2} = 0$$

$$\eta(x) = 0$$

$$-\tau\psi(x) - \xi_0^2\frac{d^2\psi}{dx^2} = 0$$

$$\tau > 0 \rightarrow \psi \sim \exp(ikx)$$

delocalized solution

$$\tau < 0$$

no delocalized solutions

$$-\tau\psi(x) + \eta(x)\psi(x) - \xi_0^2 \frac{d^2\psi}{dx^2} = 0$$

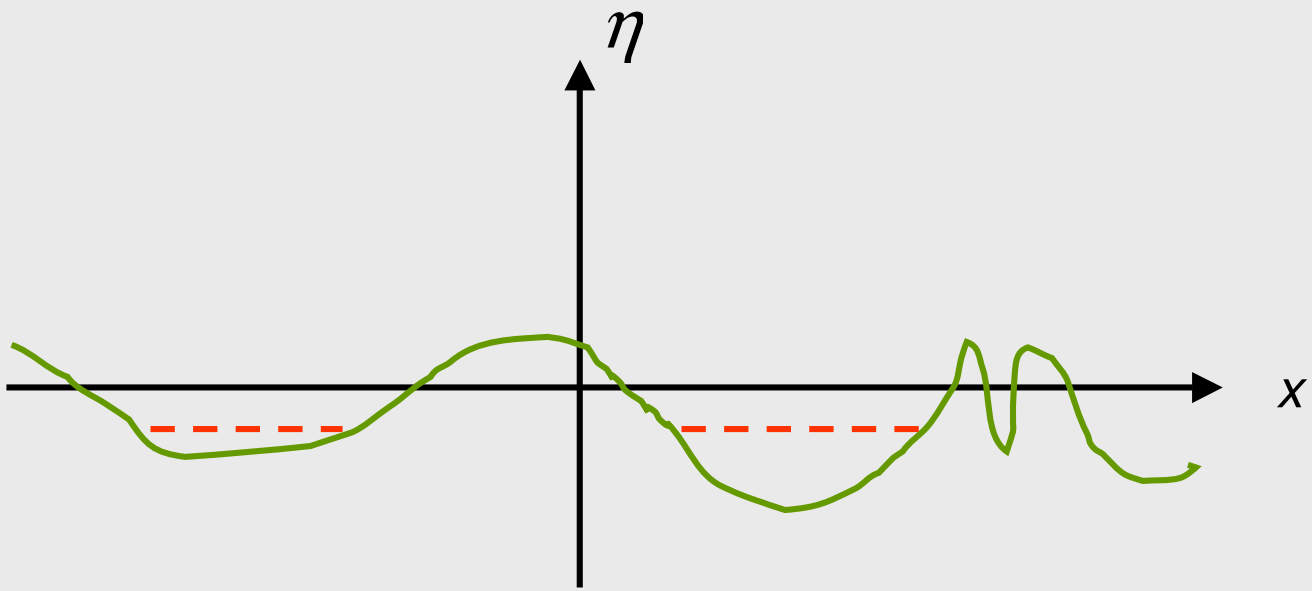

Long-range order -- mobility edge

$$-\tau A_{\mu j} + A_{\mu l}\eta_{lj}(\mathbf{r}) - \frac{3}{5}\xi_s^2\left(\frac{\partial^2 A_{\mu j}}{\partial x_l^2} + 2\frac{\partial^2 A_{\mu l}}{\partial x_l \partial x_j}\right) = 0$$

$$\eta_{jl}^{(1)}(\mathbf{r}) = -\frac{\rho^2}{r^2}\hat{\nu}_j\hat{\nu}_l \ln\left[\tanh\left(\frac{r}{2\xi_0}\right)\right]$$

D. Rainer and M. Vuorio, J. Phys. C: Solid State Phys., **10** (1977) 3093 .

$$\eta^{(1)} \sim \frac{\rho^2}{\xi_0^2} \ll 1$$

$$\eta_{jl}(\mathbf{r}) = \sum_s \eta_{jl}^{(1)}(\mathbf{r} - \mathbf{r_s})$$

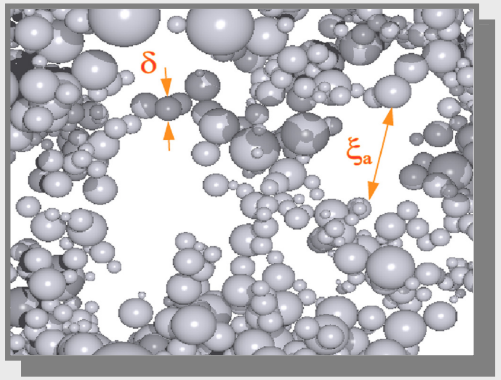

DLCA simulation of a silica aerogel depicting the length scales δ and ξ_a (courtesy of T.M. Lippman).

Perturbation expansion

$$\langle G_{mn}(\tau;\mathbf{k},\mathbf{k}')\rangle = (2\pi)^3\delta(\mathbf{k}-\mathbf{k}')\delta_{mn}G(\tau;\mathbf{k})$$

$$G(\tau;\mathbf{k}) = \frac{1}{\tau - \xi_0^2 k^2 - \Sigma(\tau,\mathbf{k})}$$

average over realizations

$\Sigma(\tau,\mathbf{k})$ =

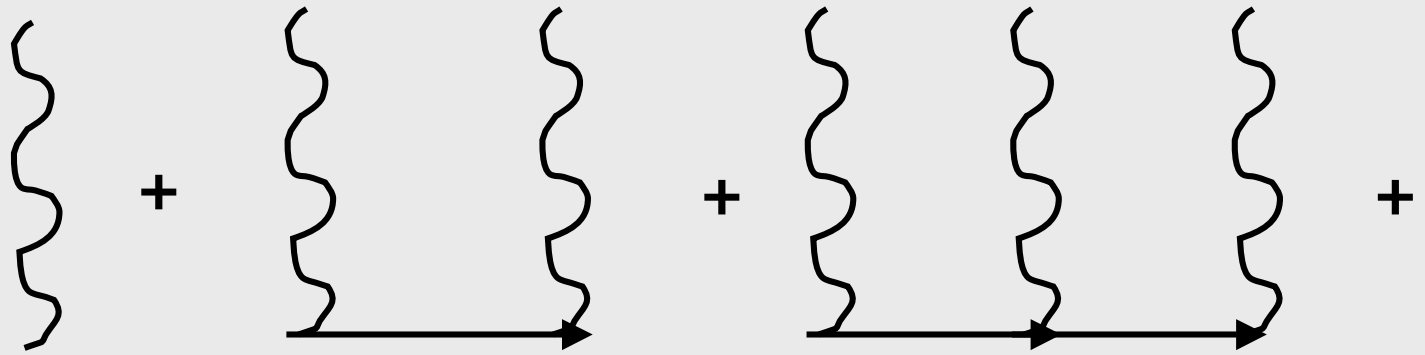

mobility edge: k=0

$$\tau = \Sigma(\tau,0)$$

$$\langle \eta_{jl}(\mathbf{k}-\mathbf{k}') \rangle = \eta^{(1)}_{jl}(\mathbf{k}-\mathbf{k}') \langle \sum_a e^{i(\mathbf{k}'-\mathbf{k})\mathbf{r}_a} \rangle$$

$$\langle \sum_a e^{i(\mathbf{k}'-\mathbf{k})\mathbf{r}_a} \rangle = (2\pi)^3 \delta(\mathbf{k}-\mathbf{k}') n$$

$$\eta^{(1)}_{jl}(\mathbf{k}=0) = \frac{\pi^3}{3}\rho^2\xi_0$$

$$\frac{4}{3}\pi\rho^2 n = \frac{1}{l_{tr}}$$

$$\tau^{(1)}_{ba} = \frac{T_b - T_a}{T_b} = \frac{\pi^2}{4}\frac{\xi_0}{l_{tr}}$$

Coincides with the homogeneous scattering model

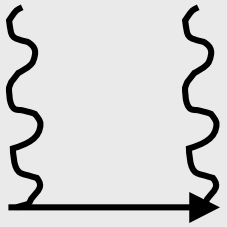

$$\tau_{ba}^{(2)} \sim \int \eta^{(1)}(\mathbf{k}-\mathbf{k_1})\eta^{(1)}(\mathbf{k_1}-\mathbf{k'})\langle \sum_{a,b} e^{i(\mathbf{k_1}-\mathbf{k})\mathbf{r}_a} e^{i(\mathbf{k'}-\mathbf{k_1})\mathbf{r}_b}\rangle G(\mathbf{k_1})\frac{d^3k_1}{(2\pi)^3}$$

$$\langle \sum_{a,b} e^{i(\mathbf{k_1}-\mathbf{k})\mathbf{r}_a} e^{i(\mathbf{k'}-\mathbf{k_1})\mathbf{r}_b}\rangle = (2\pi)^3\delta(\mathbf{k}-\mathbf{k'})n\langle \sum_{a-b} e^{i(\mathbf{k_1}-\mathbf{k})\mathbf{r}_{ab}}\rangle$$

$$\langle \sum_{a-b} e^{i(\mathbf{k_1}-\mathbf{k})\mathbf{r}_{ab}}\rangle \equiv S(\mathbf{k_1}-\mathbf{k})$$

$$\tau_{ba}^{(2)} = n\eta^{(1)}(0)\eta^{(1)}(0)\int S(k_1)G(k_1)\frac{d^3k_1}{(2\pi)^3}$$

$$G(k_1) = -\frac{5}{2\xi_0^2 k_1^2}$$

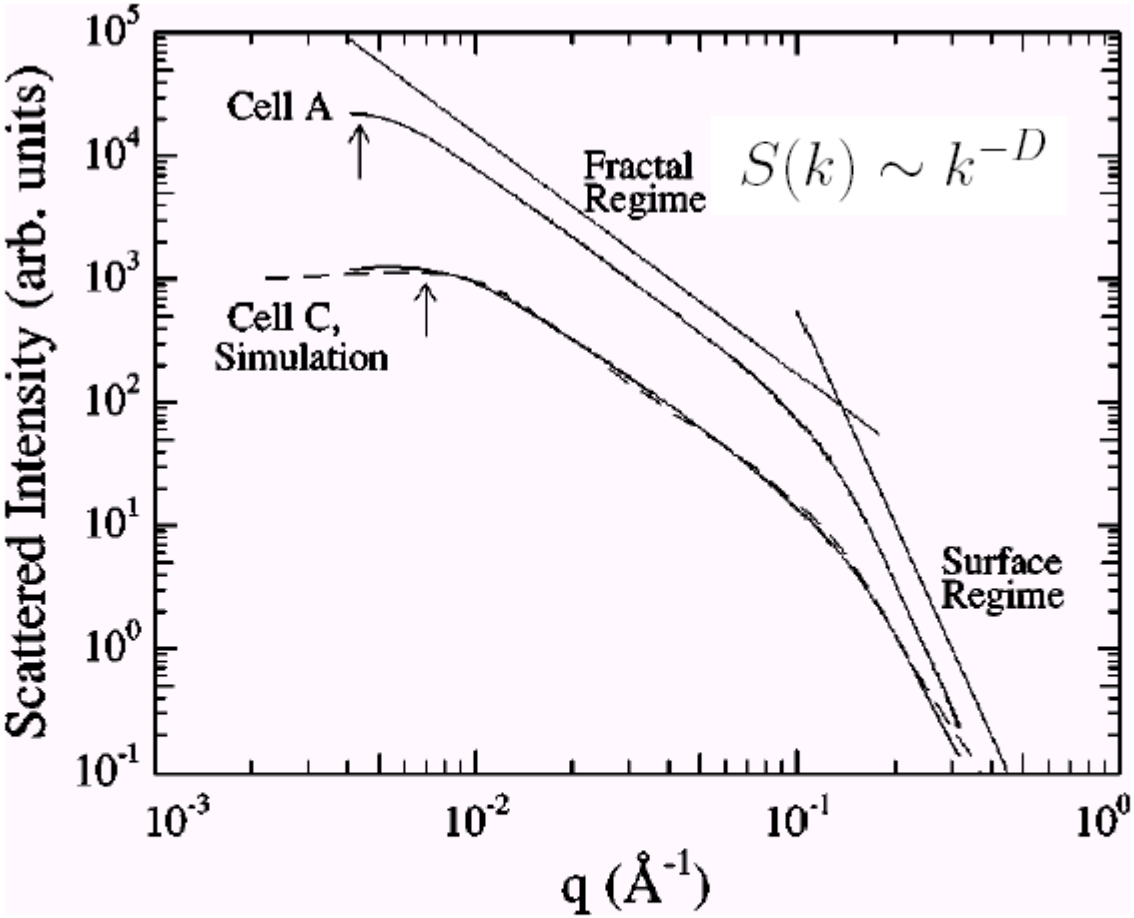

FIG. 1. Small-angle x-ray scattering from two different aerogels. The upper solid curve is for the aerogel sample from cell A and the lower solid curve is for the aerogel from cell C. (Both samples were 98.2% open). The dashed line is the scattered inten-

Fractal structure (Sierpinski gasket)

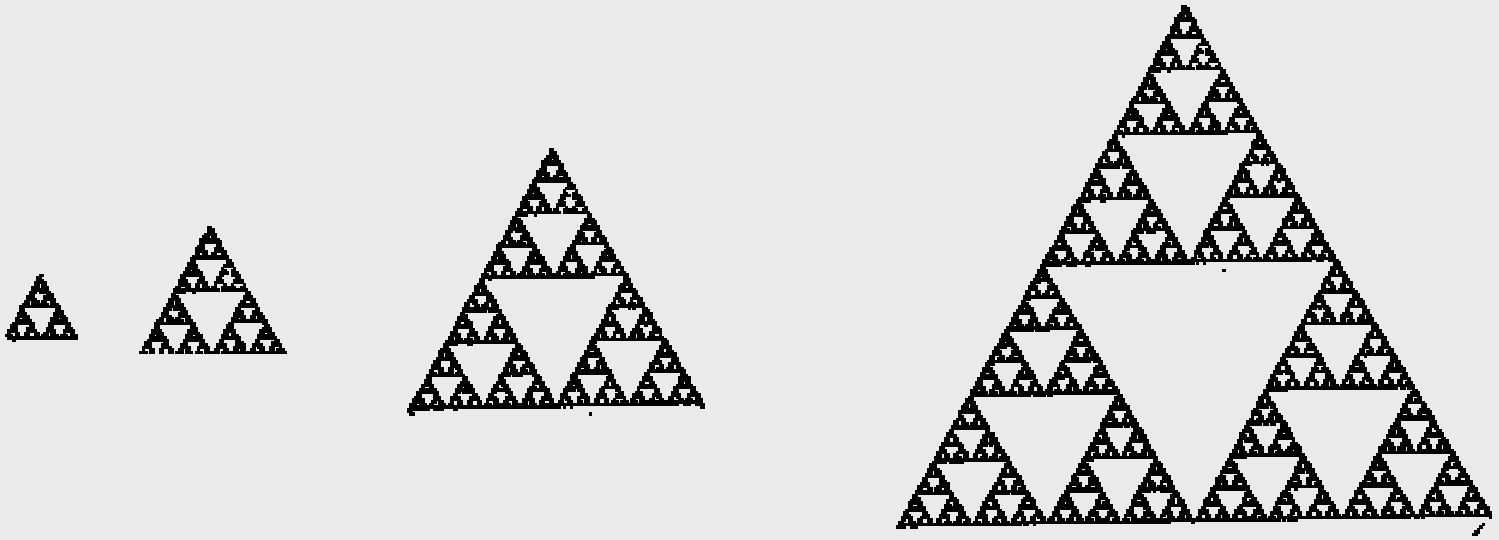

$$M(L) \sim L^D$$

$$D = \frac{\ln 3}{\ln 2} \approx 1.5849$$

$$S(k) \sim k^{-D}$$

$$k_{min} \ll k \ll k_{max}$$

$$k_{min} \approx \frac{1}{R}$$

$$k_{max} \approx \frac{1}{\rho}$$

$$\tau_{ba}^{(2)} = n\eta^{(1)}(0)\eta^{(1)}(0) \int S(k_1)G(k_1)\frac{d^3k_1}{(2\pi)^3}$$

$$S(\mathbf{k}) \sim \frac{nR^3}{(kR)^D}$$

$$\tau_{ba}^{(2)} = -(n\eta^{(1)}(0)^2 A\frac{R^3}{\xi_0^2} \int \frac{dk}{(kR)^D}$$

$$D \approx 1.8$$

$$\tau_{ba} = \frac{\pi^2}{4}\frac{\xi_0}{l_{tr}} - \left(\frac{\pi^2}{4}\frac{\xi_0}{l_{tr}}\right)^2 B\left(\frac{R}{\xi_0}\right)^2$$

$$\frac{\xi_0}{l_{tr}}\left(\frac{R}{\xi_0}\right)^2 \sim 1$$

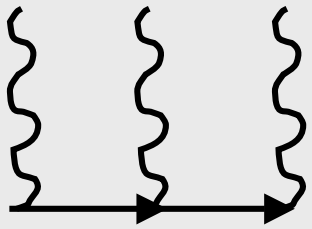

$$\tau_{ba}^{(3)} \sim n(\eta^{(1)}(0))^3 \int \frac{d^3k_1}{(2\pi)^3}\frac{d^3k_2}{(2\pi)^3} G(k_1)G(k_2)\langle \sum e^{i\mathbf{k_1}\mathbf{r}_{ab}} e^{i\mathbf{k_2}\mathbf{r}_{ca}} \rangle$$

$$\langle \sum e^{i\mathbf{k_1}\mathbf{r}_{ab}} e^{i\mathbf{k_2}\mathbf{r}_{ca}} \rangle = S(\mathbf{k_1})S(\mathbf{k_2})$$

$$\tau_{ba} = \frac{\tau^{(1)}}{1+\tau^{(1)}Q}$$

$$Q = \int S(k_1)G(k_1)\frac{d^3k_1}{(2\pi)^3}$$

$$\tau_{ba} = \frac{\frac{\pi^2}{4}\frac{\xi_0}{l_{tr}}}{1 + \left(\frac{\pi^2}{4}\frac{\xi_0}{l_{tr}}\right) B \left(\frac{R}{\xi_0}\right)^2}$$

$R \ll \xi_0$

HSM

$\frac{\xi_0}{l_{tr}} \left(\frac{R}{\xi_0}\right)^2 \gg 1$

$\tau_{ba} \sim \left(\frac{\xi_0}{R}\right)^2$

$x = \frac{\xi_0}{2l}$

$\zeta_a = \frac{\pi R}{2\sqrt{2}l}$

$x \to \tilde{x} = \frac{x}{1 + \zeta_a^2/x}$

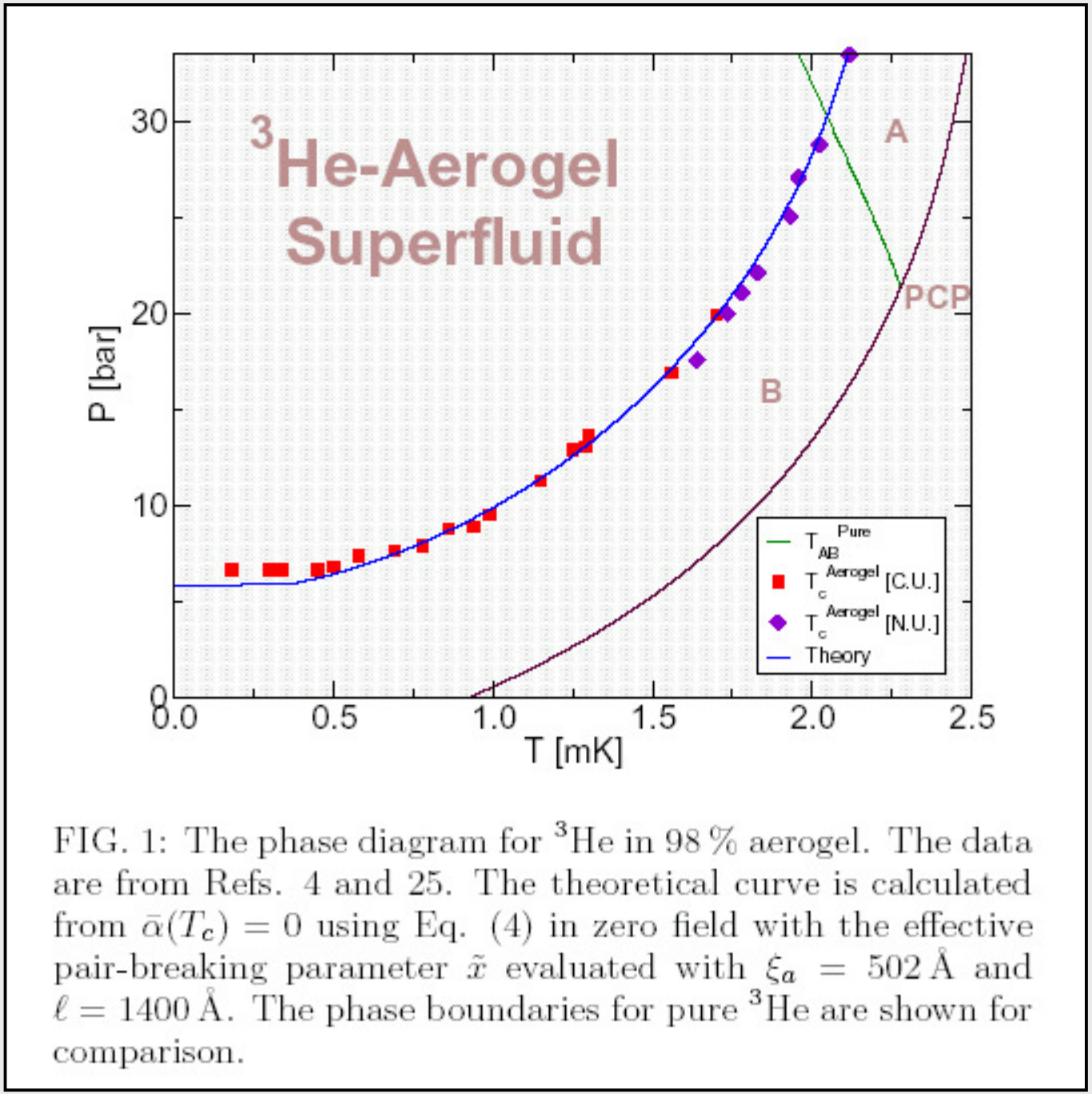

FIG. 1: The phase diagram for ^{3}He in 98 % aerogel. The data are from Refs. 4 and 25. The theoretical curve is calculated from $\bar{\alpha}(T_c) = 0$ using Eq. (4) in zero field with the effective pair-breaking parameter $\tilde{x}$ evaluated with $\xi_a = 502\,\text{Å}$ and $\ell = 1400\,\text{Å}$. The phase boundaries for pure ^{3}He are shown for comparison.

Conclusions

1. It is possible to introduce impurities in the superfluid 3He.

2. Effect of impurities depends on correlation of their positions.

3. One can expect effects, analogous to discussed here in unconventional superconductors with a short correlation length, e.g. in high-Tc superconductors.

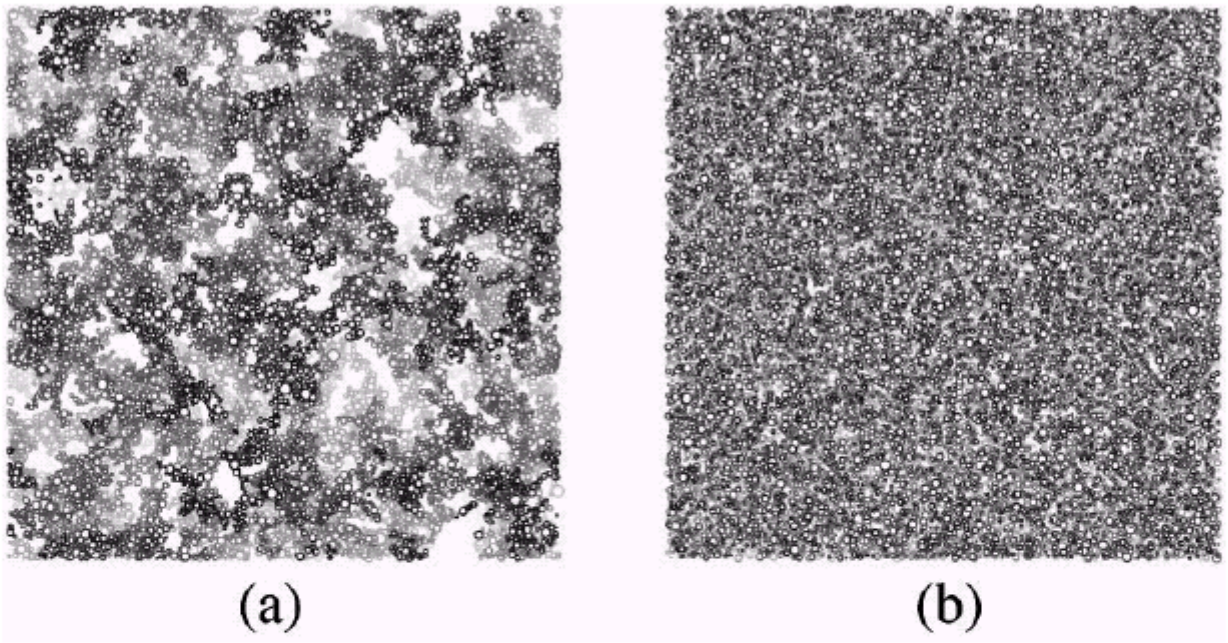

FIG. 2. Panel (a) shows the projection of a cube of aerogel, $\simeq 3500$ Å on a side, simulated with the DLCA model. The aerogel has a volume concentration of 0.018 (98.2% open). The particle diameters have a Gaussian distribution around $\simeq 30$ Å, with width $\sigma = 15$ Å. The particles are plotted on a gray scale according to their z position, with the darkest in the foreground. For comparison

Superfluidity of ^{4}He
(P.L. Kapitza 1937).

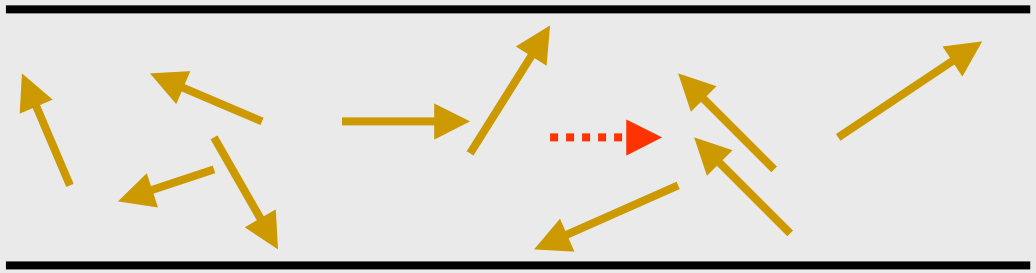

classical flow

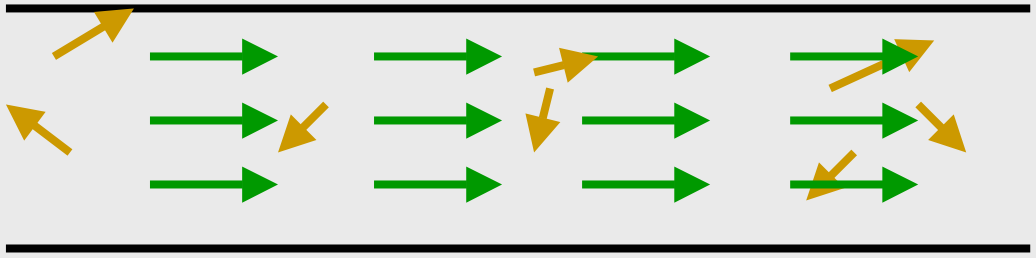

Superflow – ordered (coherent) flow.
No enthropy is carried by the superfluid part.

$$T_\lambda = 2.17K$$

Structure & Correlations

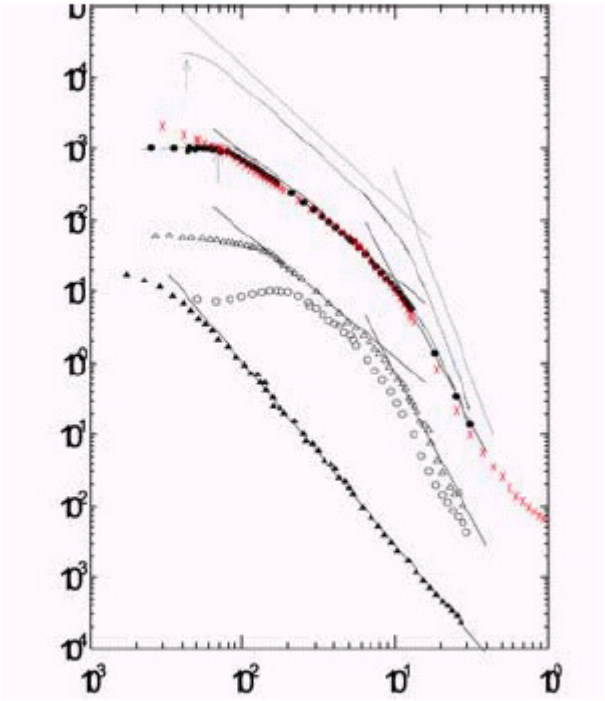

Aerogels exhibit fractal correlations.

- •99.5% open base catalysed aerogel (Larry Luria)
- Δ 96% open base catalysed aerogel
- o 91% open base catalysed aerogel
- ▲95.6% neutrally catalysed aerogel

Cell A, C ~98% open aerogel

J. V. Porto, PhD. Thesis, Cornell (1996)[4]

$$-\tau A_{\mu j}+A_{\mu l}\eta_{lj}(\mathbf{r})-\frac{3}{5}\xi_s^2\left(\frac{\partial^2 A_{\mu j}}{\partial x_l^2}+2\frac{\partial^2 A_{\mu l}}{\partial x_l \partial x_j}\right)+\frac{1}{2}\sum_{p=1}^{5}\beta_p\frac{\partial I_p}{\partial A^*_{\mu j}}=0$$

$$\xi_0 \to \infty$$

$$\tau_a^{(1)}\delta_{jl}=<\eta_{jl}>=\frac{\pi^2}{12}\frac{\xi_0}{l_{tr}}\delta_{jl}=\frac{\pi^2}{12}\frac{\xi_0}{\rho}(1-P)\delta_{jl}$$

$$C(r)=n\frac{D}{3}\left(\frac{R}{r}\right)^{3-D}$$

$$S(k)=\frac{4\pi D}{3}n\frac{R^{3-D}}{k^D}\int_0^1\frac{\sin x}{kr}x^{2-D}dx$$

$$\tau_{ba}^{(2)}=-(n\eta^{(1)}(0))^2 A\int\frac{1}{(kR)^D}\frac{5}{2\xi_0^2k^2}\frac{4\pi k^2 dk}{(2\pi)^3}$$

$$S(\mathbf{k}) = \langle \sum_{a-b} e^{i\mathbf{k}\mathbf{r}_{ab}} \rangle = \int C(\mathbf{r}) e^{i\mathbf{k}\mathbf{r}} d^3 r$$

$$G(\tau; \mathbf{k}, \mathbf{k}') = \frac{(2\pi)^3 \delta(\mathbf{k} - \mathbf{k}')}{\tau - (2/5)\xi_0^2 k^2 - \Sigma(\tau, \mathbf{k})}$$

$$-\tau A_{\mu j} + A_{\mu l}\eta_{lj}(\mathbf{r}) - \frac{2}{5}\xi_0^2 \left(\frac{\partial^2 A_{\mu j}}{\partial x_l^2}\right) = 0$$

$$\eta_{jl}(\mathbf{r}) = \sum_s \eta_{jl}^{(1)}(\mathbf{r} - \mathbf{r_s})$$

$$\eta_{jl}^{(1)}(\mathbf{r}) \sim (\rho/\xi_0)^2$$

$$\eta_{jl}^{(1)}(\mathbf{r}) = -\frac{\rho^2}{r^2}\hat{\nu}_j \hat{\nu}_l \ln\left[\tanh\left(\frac{r}{2\xi_0}\right)\right]$$

$$r \leq \xi_0$$

^{4}He and ^{3}He are QUANTUM LIQUIDS

At T$\sim$1 K thermal De-Broigle wave-length $\lambda_T = \frac{2\pi\hbar}{\sqrt{2mT}}$ is of the order of the interatomic distance a

1. At normal pressure both ^{4}He and ^{3}He do not solidify down to T=0.

2. Statistics is important:

   $^4\mathrm{He} = (2p + 2n + 2e)$: Bose-liquid

   $^3\mathrm{He} = (2p + 1n + 2e)$: Fermi-liquid

Modified HSM Model (Sharma & Sauls)

When $\xi_{3He} \sim \xi_a << l$ *(mfp)*, T_c set by most dense regions $\delta T_c/T_{co} \sim -(\xi_{3He}/\xi_a)^2$.

When $\xi_{3He} >> \xi_a << l$ *(mfp)*, $\delta T_c/T_{co} \sim -(\xi_{3He}/l)$.

Within this heuristic model, Sauls and Sharma find good agreement between Tc, with a fixed mean free path ξ_a=502Å, l=1400Å.

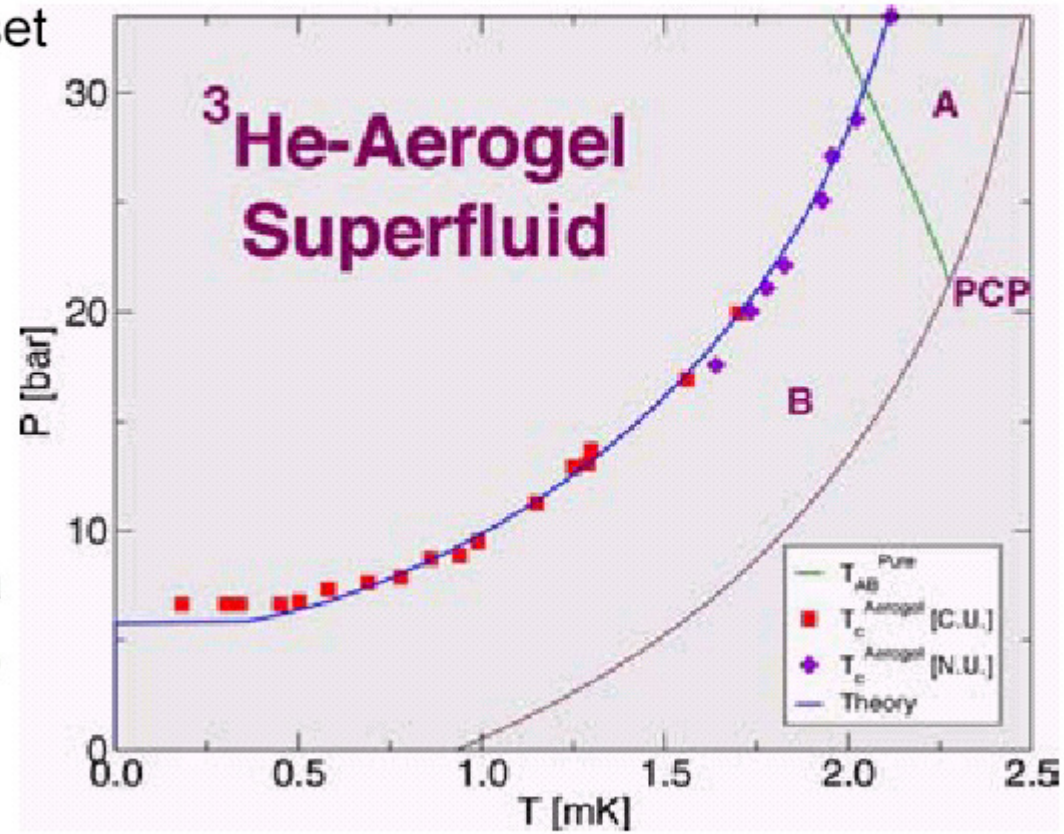

Sharma & Sauls, PRB **68**224500 (2003).